J. exp. Biol. 172, 387-402 (1992)
Printed in Great Britain © The Company of Biologists Limited 1992

CIRCUIT ANALYSIS OF TRANSMEMBRANE VOLTAGE RELATIONSHIPS IN V-ATPase-COUPLED ION MOVEMENTS

BY FRANCIS G. MARTIN

Department of Biology, Immaculata College, Immaculata, PA 19345, USA

Summary

The concept of electrical circuit analysis is extended to include components found in membrane ionic transport systems. As in classical electrical equivalent circuits, resistors and capacitors are used to represent ion channels and the membrane capacitances, respectively; batteries represent energy sources driven by chemical reactions. In the extensions proposed, energy stored in various ionic concentrations is treated as charges on compartmental capacitors; symporters and antiporters are treated as energy-coupling devices analogous to transformers in alternating current electrical circuits. Pumps are shown to be special cases of porters in which the input circuit derives its energy from a chemical reaction. Using these components, circuit diagrams are drawn for several examples of membrane ion transport systems. By applying appropriate circuit analysis techniques, these diagrams facilitate the quantitative description of the energy distributions throughout the system.

Introduction

Models of membrane-associated ionic events have long provided a conceptual framework for organizing and communicating data obtained from real systems. Such models usually take the form of equivalent electrical circuits which can be subjected to standard electrical circuit analysis techniques to describe quantitatively the voltage and current relationships among the components.

Probably the most familiar of the equivalent electrical circuits is the model of the squid giant axon used by Hodgkin and Huxley (1952) to describe the ionic events associated with the generation of nerve action potentials. Finkelstein and Mauro (1963) extended the use of equivalent electrical circuits to model membrane systems and developed the concept of the pure electrical equivalent of the membrane. The models proposed by Hodgkin and Huxley and by Finkelstein and Mauro considered only the movement of ions down their electrochemical gradients. Several years elapsed before electrogenic ion pumps were included in the equivalent electrical circuits (e.g. Kishimoto *et al.* 1981).

The analysis of equivalent electrical circuit models has proved useful in studying transmembrane ionic movements associated with transient events, like sensory receptor potentials (Martin and Mote, 1980) and action potentials, which do not significantly affect the transmembrane ionic gradients. By contrast, in the complex world of porters, pumps and channels, the application of circuit analysis techniques has been scant. This

Key words: ionic circuits, compartmental capacitance, ionic pumps, cotransporters, ion-transporting ATPases.

paper proposes an extension of electrical circuit analysis technique to model ionic systems typical of biological plasma membranes in single cells and epithelia. The fundamental techniques of circuit analysis include Ohm's law, Kirchhoff's laws, the Thevenin and Norton theorems, as well as mesh and nodal network analysis (e.g. Edminister, 1965). These techniques are as applicable to ionic systems as they are to electrical systems. However, ionic circuits are characterized by a multiplicity of current carriers, by energy coupling between carriers, and by energy storage being distributed between ionic activity gradients and the membrane capacitance. For these complex circuits the definitions of some components have been refined. The components and their assembly into ionic circuits is discussed.

Circuit components

Included in all equivalent electrical circuits are resistors, capacitors and batteries. Each of these electrical components represents a corresponding physical component in the membrane systems. Resistors represent the various ionic channels found in the membrane. Capacitors represent the plasma membrane with its insulating lipid core separating two conductive aqueous solutions. Batteries represent ionic gradients having an electromotive force (emf) equal to the corresponding Nernst equilibrium potential. However, symporters, antiporters and pumps do not have a typical component designation in their own right, but are usually represented as constant current or constant voltage generators in most electrical equivalent circuits (Läuger, 1991).

In the present analysis, resistors and capacitors are used to represent ionic pathways and membrane capacitances in the usual way. Batteries, however, are restricted to instances where chemical bonds are broken to generate a fixed emf or, more appropriately, an ion-motive force (imf), related to the free energy of the reaction. The ion activity gradients, porters and pumps are treated in a novel way using the concept of compartmental capacitance.

Compartmental capacitances

The storage of energy in activity gradients presents a conceptual problem. The usual method of representing them as batteries is particularly awkward. Ideal batteries have a constant output potential determined by the free energy of the chemical reaction involved. As batteries discharge, the open-circuit potential of the battery remains constant whereas the closed-circuit output voltage decays. This condition can be schematized by including an internal resistance in series with an idealized battery. As the battery discharges, the amount of substrate decreases and the overall rate of the reaction decreases, raising the effective internal resistance. The discharge of an activity gradient is not like the discharge of a battery. When a gradient discharges, withdrawal of energy actually decreases the magnitude of the free energy involved, a condition more like the discharging of a capacitor than that of a battery.

The capacitance (C) of a device is mathematically defined as the ratio of a change in charge (dQ) to the resulting change in electrical potential (dE):

$$C = dQ/dE. \tag{1}$$

For any given ionic species, k (following the terminology of Snell *et al.* 1965), dQ_k can, in turn, be defined in terms of the change in the number of ions (dN_k) in a compartment:

$$dQ_k = Z_k F \times dN_k, \tag{2}$$

where z is the valency and F is Faraday's constant. The compartmental dE_k for a given dN_k can be determined by the Nernst equation (for simplicity we will consider no change in compartmental volume or ionic activity coefficient):

$$dE_k = \frac{\boldsymbol{RT}}{Z_k F} \times \ln \frac{N_k}{N_k + dN_k}, \tag{3}$$

where $\boldsymbol{R}$ is the gas constant and T is absolute temperature. By combining equations 1, 2 and 3, an equation for the ionic compartmental capacitance can be written:

$$C_k = \frac{F^2}{\boldsymbol{RT}} \times Z_k^2 \times dN_k / \{\ln[N_k/(N_k + dN_k)]\}. \tag{4}$$

From numerical analysis, it can be shown that as dN_k approaches zero

$$C_k \text{ approaches } \frac{F_2}{\boldsymbol{RT}} \times Z_k^2 \times N_k. \tag{5}$$

If activity (A_k) is used to express the number of ions present, then the ionic compartmental capacitance can be shown to be directly proportional to the volume (v) of the compartment and inversely proportional to the activity coefficient (a_k) for the ion:

$$C_k = \frac{F^2}{\boldsymbol{RT}} \times Z_k^2 \times A_k \times \frac{v}{a_k}. \tag{6}$$

Compartments with large volumes and small activity coefficients will have larger ionic compartmental capacitances than smaller compartments with large activity coefficients for the ion of interest. Moreover, the ionic compartmental capacitance is not a constant but varies proportionally with the number or activity of ions in the compartment. This dependency on the number of ions in the compartment must be considered, and further explored, when considering significant perturbations in the system.

A membrane always separates two compartments. If each compartment has an ionic compartmental capacitance for each ionic species involved then a total ionic compartmental capacitance for a two-compartment system can be determined (again, for simplicity assume no change in compartmental volume or ionic activity coefficient).

The total ionic compartmental capacitance (Ct_k) of the two-compartment system can be calculated by first determining the change in equilibrium potential as ions move from the outside (o) compartment to the inside (i) compartment:

$$dE_k = \frac{\boldsymbol{RT}}{Z_k F} \times \ln \frac{No_k(Ni_k + dN_k)}{Ni_k(No_k - dN_k)} \tag{7}$$

(for the derivation of this equation see Appendix 1).

Then, by finding the ratio between the change in voltage and the change in charge:

$$Ct_k = \frac{F^2}{RT} \times Z_k^2 \times dN_k / \ln\{[No_k(Ni_k + dN_k)]/[Ni_k(No_k - dN_k)]\} . \quad (8)$$

From numerical analysis, it can be shown that as dN_k approaches zero:

$$Ct_k \text{ approaches } \frac{F^2}{RT} \times Z_k^2 \times \frac{No_k Ni_k}{No_k + Ni_k} . \quad (9)$$

Exactly this same equation is obtained when the inside and outside ionic compartmental capacitances are in series with each other (see Appendix 2).

In cases where just two compartments are separated by a membrane (e.g. vesicles in cytoplasm or vesicles in a bath) it is probably more convenient to lump both ionic compartmental capacitances into a single combined capacitance. Since, in most cases, the vesicular or cellular volume will be much smaller than the cytoplasmic or bath volume, respectively, the vesicular or cellular ionic compartmental capacitances will be very close to the combined ionic capacitance. When considering epithelia, which are, by definition, polycompartmental systems (at least lumen, intracellular space and blood), it is necessary to consider the ionic capacitances of each compartment individually since each compartment can be ionically coupled to more than one other compartment by ionic transport mechanisms.

Porters and pumps

Symporters and antiporters are commonly thought of as current-coupling devices. They are often defined in terms of their coupling ratios of 1:1, 2:1, 3:2, etc. But they can also be thought of as energy-coupling devices. Energy delivered to the device by an ionic current will be dissipated by the device. The dissipated energy can take two forms: energy lost as heat and energy used to do work. In the ideal porter, no energy would be lost as heat and all the energy delivered by an ionic current would be used to do work. When the work done is to generate an imf for a secondary ionic species, the relationship between the primary and secondary ionic species is analogous to the relationship between the primary and secondary coils in an a.c. transformer. The current, voltage and impedance relationships for porters will be described using this transformer analogy.

Fig. 1A shows the circuit symbol for porters used in this paper. It was derived from the typical symbol used to represent coupling devices in membrane diagrams (Fig. 1B); its origins can be traced back at least as far as Hodgkin and Keynes (1955). Input and output circuits are arbitrarily assigned in the ideal coupler, i.e. the ideal porter is considered reversible. The coupling coefficient (m) is considered positive if the input and output currents through the device are in opposite directions.

If we assume that the porter is ideal, then power delivered in the input circuit (P_{in}) will equal the power dissipated in the output circuit (P_{out}):

$$P_{in} = P_{out} \quad (10)$$

and the current coupling ratio (m) will be defined as:

$$m = I_{in}/I_{out} . \quad (11)$$

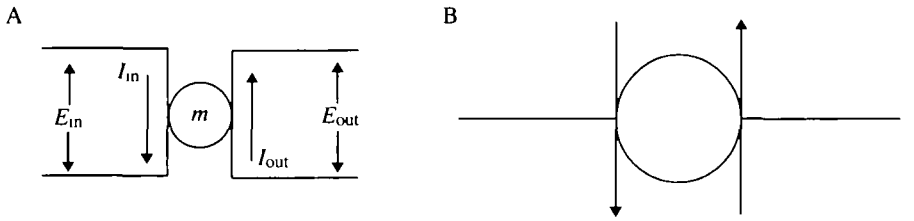

Fig. 1. (A) The circuit symbol for an ideal porter. (B) Diagram of a porter after Hodgkin and Huxley (1955).

It can be shown that (see Appendix 2 for derivations):

$$m = E_{out}/E_{in} \tag{12}$$

and

$$m^2 = R_{out}/R_{in}\,, \tag{13}$$

where R is resistance.

This analysis yields the following relationships. Anion/anion or cation/cation antiporters would have positive coupling coefficients. Anion/anion or cation/cation symporters would have negative coupling coefficients. Anion/cation antiporters would have negative coupling coefficients whereas anion/cation symporters would have positive coupling coefficients. This definition of the coupling ratio simplifies mesh analysis of the ionic circuits and is consistent with the definition of positive current as the passive movement (i.e. downhill movement driven by ionic electrochemical gradients) of positive ions into cells. By implication, the active movement (i.e. uphill movement driven directly or indirectly by metabolic processes) of positive ions out of cells is also positive current.

For a more realistic depiction of porters, it is necessary that frictional losses of the porter mechanism and also possible 'slip' of ions through the mechanism without accompanying coupling be considered. Frictional losses can be modeled by adding a resistance (R_S) in series with either the input or output sides of the porter. Slippage can be modeled by adding a resistance in parallel (R_P) with either the input or the output side of the porter. Exactly where these resistances are placed depends on what is known about the particular porter being modeled and the degree to which a faithful representation of the mechanism is desired. The impedance coupling relationship (equation 13) ensures that appropriate values placed on either side will have an equivalent value on the opposite side (see Fig. 2).

Pumps are special cases of porters. The input side of a pump is driven by the free energy, expressed in volts, of the chemical reaction (usually ATP hydrolysis) driving the pump, i.e. the pump potential (V_P). The pump coupling coefficient (m_k) is the ratio of the number of energy substrate molecules split to the number of ions pumped. Fig. 3A depicts an ideal pump whereas Fig. 3B depicts a more realistic pump with frictional and slippage resistances added. All power, current, voltage and impedance relationships hold for pumps as they do for porters.

In order to determine the relationship between V_P and imf for the pumping mechanism

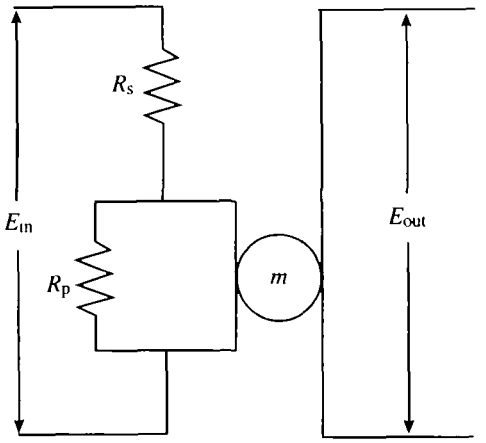

Fig. 2. The circuit symbol for a porter with friction and slippage.

shown in Fig. 3B, the total load on V_p must be determined. First let R_l be the impedance (resistance in this case) offered by the porter. This value can be determined by substituting circuit components into equation 13:

$$R_l = R_k/m_k^2 . \tag{14}$$

Then let R_2 be the parallel combination of the input side of the porter and the slip/leakage resistance R_p:

$$R_2 = \frac{R_p \times R_l}{R_p + R_l} . \tag{15}$$

R_2 forms a voltage divider with R_s, dropping a portion of the pump potential across the input side of the porter. The output side of the porter (the imf) is related to the input potential by equation 12. Combining all these equations yields the desired relationship:

$$\text{imf} = V_p \times m_k \times \frac{R_2}{R_2 + R_s} . \tag{16}$$

Sample circuits (corresponding to the models in Harvey, 1992)

Example 1: a proton pump in a vesicular membrane

An extremely simple system consisting of a pump for a single ionic species in a membrane separating two aqueous compartments (Fig. 4A) is considered first. Based on

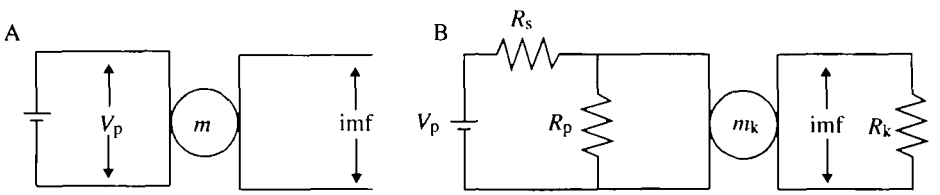

Fig. 3. (A) The circuit symbol for an ideal pump. (B) A realistic pump circuit with internal losses.

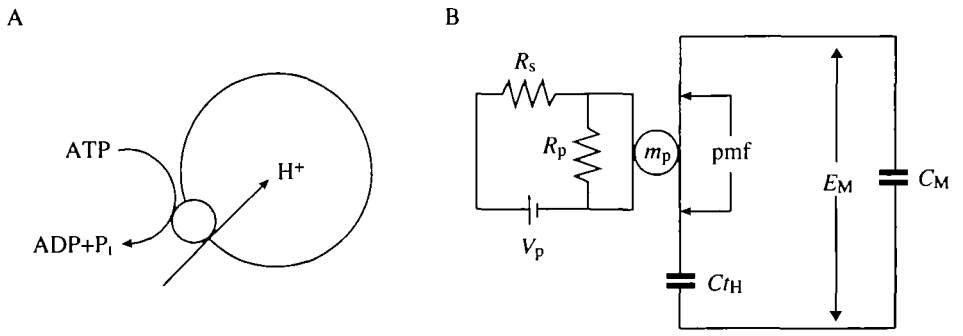

Fig. 4. (A) A proton pump in a vesicle membrane (example 1). (B) Circuit diagram for example 1.

this hypothetical situation the circuit shown in Fig. 4B can be drawn. In the circuit, the ionic (in this case, proton) pump is depicted by the V_p/porter combination. For the purposes of these analyses the frictional and slippage resistances are considered to be negligible and are ignored. In the steady state, in this case equilibrium, the pump will generate a proton-motive force (pmf) which is the product of the pump potential (V_p) and the proton porter coupling coefficient (m_p):

$$\text{pmf} = V_p \times m_p . \tag{17}$$

The pmf will be dropped across the series combination of the membrane capacitance (C_M) and the total proton compartmental capacitance (Ct_H). The proportion of the pmf dropped by each capacitance is related to the size of each capacitor. The voltage drop across C_M is the membrane potential (E_M) and its relationship to the other components in the system is given by:

$$E_M = V_p \times m_p \times \frac{Ct_H}{Ct_H + C_M} . \tag{18}$$

The Nernst proton equilibrium potential (E_H) for the system is the voltage drop across Ct_H and is the difference between E_M and the pmf:

$$E_H = E_M - \text{pmf} . \tag{19}$$

The voltage relationships in this circuit point out two interesting facets. If Ct_H is large with respect to C_M then the pmf will be dropped mostly across the membrane capacitance and the proton pump will look like a potential generator. If Ct_H is small with respect to C_M then the pmf will drop mostly across the proton compartmental capacitance and the proton pump will look like a pH gradient generator. A small Ct_H at a typical pH for a vesicle would necessitate a very small volume and a large activity coefficient. Hence, whereas quite large membrane potentials could be developed depending on the m_p, it would be difficult to imagine a proton pump alone being responsible for significant acidification of a vesicular compartment.

Example 2: a proton pump in a vesicular membrane with gegenion leakage

To acidify a compartment significantly the value of the effective membrane capacitance must be close to, or greater than, the proton compartmental capacitance. This condition can be achieved by adding a channel for a non-pumped ionic species (i.e. a gegenion), which moves under the influence of the membrane potential and its own activity gradient only. A gegenion channel is included in the system shown in Fig. 5A,B. In this circuit the E_M is the sum of two voltages: the voltage drop across the gegenion resistance (R_k) and that of the total gegenion compartmental capacitance Ct_k. In the steady state no current will flow through R_k, effectively putting Ct_k and C_M in parallel. The equilibrium relationship of the membrane potential to the other components of the system is described by equation 20:

$$E_M = V_p \times m_p \times \frac{Ct_H}{Ct_H + C_M + Ct_k}, \tag{20}$$

$$E_k = E_M, \tag{21}$$

$$E_H = E_M - \text{pmf}. \tag{22}$$

In this example, acidification is made possible because the larger capacitors dominate the system in the steady state. Since both the protons and the gegenions occupy the same compartments, it is reasonable to assume that the compartmental capacitances for the two ions will be similar. In this situation, significant charging of the proton compartmental capacitance could be effected by the proton pump. It makes no difference whether the gegenion is an inwardly moving anion like chloride or an outwardly moving cation like sodium. Either can increase the effective steady-state membrane capacitance of the system and cause development of a pH gradient with the inside of the vesicle being acid with respect to the bath.

Example 3: a vesicular membrane with a proton pump, a porter and gegenion leakage

A proton pump can be used to make a compartment alkaline if its energy is used to drive an ionic cotransporter and the effective membrane capacitance is made correspondly large by passive gegenion movement. Diagrams for this circuit can be seen

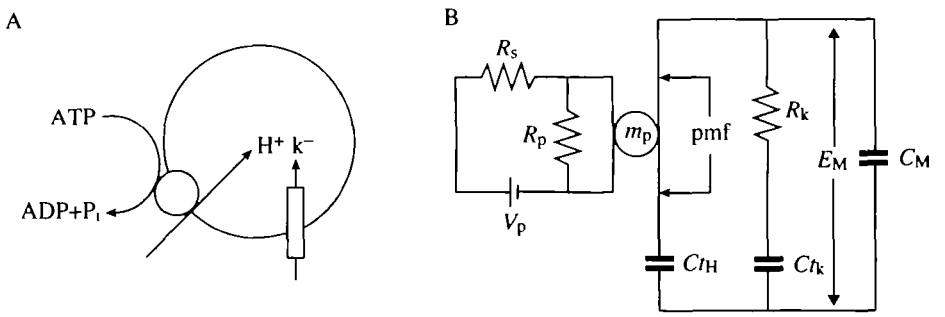

Fig. 5. (A) A proton pump in a vesicular membrane with a gegenion leakage (example 1). (B) Circuit diagram for example 2.

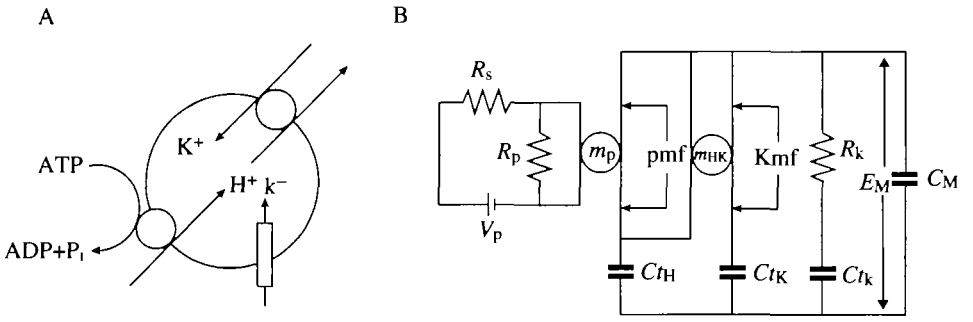

Fig. 6. (A) A vesicular membrane with a proton pump, an H^+/K^+ porter and a gegenion leakage (example 3). (B) Circuit diagram for example 3.

in Fig. 6A,B. In these diagrams the cotransporter transfers energy in the proton circuit to the potassium circuit. Consistent with the direction of energy transfer, the coupling coefficient is designated m_{HK}, and the cotransporter is designated an H^+/K^+ antiporter. The potassium-motive force (Kmf) is related to the pmf by:

$$\text{Kmf} = m_{HK} \times \text{pmf}\,. \tag{23}$$

The equations describing the remaining voltage relationships in the circuit can be determined by writing and solving a pair of simultaneous equations. One equation describes the voltage distributions throughout the circuit that would result if the pmf were present but the Kmf were zero. The other equation describes the voltage distributions throughout the circuit that would result if the Kmf were present but the pmf were zero. The following voltage relationships will apply when the system comes to equilibrium:

$$E_M = \text{pmf} \times \frac{Ct_H + (m_{HK} \times Ct_K)}{Ct_H + C_M + Ct_k + Ct_K}, \tag{24}$$

$$E_k = E_M\,, \tag{25}$$

$$E_H = E_M - \text{pmf}\,, \tag{26}$$

$$E_K = E_M - \text{Kmf}. \tag{27}$$

For this circuit to be effective in compartment alkalization, Ct_H would have to be relatively large with respect to Ct_K and Ct_k; this condition could be effected by buffering the compartment to bring the proton activity coefficient to very low levels while keeping the activities of the other ions involved relatively high. The increase in Ct_H brought about by buffering would increase the effective capacitance in parallel with the membrane capacitor, thereby increasing E_K. But even with significant buffering of the inside compartment m_{HK} must still be greater than 1. In order to alkalize the inside compartment with respect to the bath m_{HK} must be high enough to drive the E_H positive and this is only possible when:

$$m_{HK} > 1 + \frac{Ct_k + C_M}{Ct_k}\,. \tag{28}$$

(see Appendix 4 for derivation).

Example 4: the goblet cell in the midgut epithelium of the larval lepidopteran

This example describes a polycompartmental system; it provides a basis for a discussion of the salient points that must be considered whenever complex ion circuits are to be analyzed.

Fig. 7A describes the principal ionic pathways found in the goblet cell of the larval midgut of *Manduca sexta* (Harvey, 1992). The system represented has four compartments: the midgut lumen, the goblet cavity, the goblet cell intracellular space and the blood. A proton pump and proton/potassium antiporter are located in the membrane lining the goblet cavity. Bicarbonate, or perhaps more likely carbonate, is generated by metabolic activity and passes preferentially across the apical side of the epithelium. The

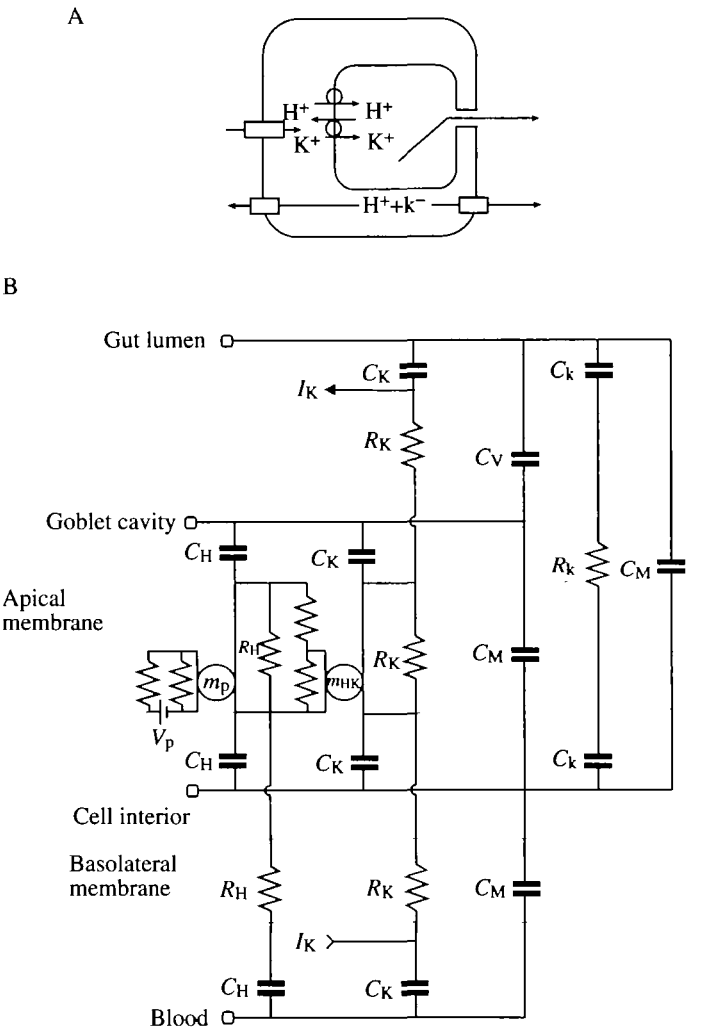

Fig. 7. (A) Ionic movement through a goblet cell. (B) Circuit diagram of a goblet cell.

apical membrane consists of the membrane lining the goblet cavity, continuing through the valve region, and across the lumen/intracellular interface.

Fig. 7B is a schematic diagram of the goblet cell system showing the component parts of the pathways shown in Fig. 7A. Each compartment has ionic compartmental capacitances associated with it: C_H, C_K and C_k. These are single compartment ionic capacitances rather then the combined compartmental capacitances used in the previous circuits of this paper. Along with the polycompartmental considerations mentioned previously, the single compartmental capacitances are used here to isolate each ionic pathway from the others. d.c. connections between the different ionic pathways do exist and will be the topic of a later publication.

Membrane capacitances are found associated with each portion of membranes where they separate different compartments; C_v is a composite capacitance for the valve assembly. Although it is probably very small and not representative of the complexity of this structure (see Moffett and Koch, 1992), it does allow the goblet cavity/lumen interface to be drawn like all the others. Membrane potentials are measured at the locations indicated by the test point circles and, hence, are only capacitatively coupled to the voltage drops associated with the ionic currents.

As drawn here, the goblet cell has a 'power take-off' in the potassium ionic circuit. Potassium currents traveling longitudinally in the lumen and the blood can drive amino acid uptake in neighboring columnar cells (see Fig. 8). These extra goblet cell pathways would add to the load on the porter and hence to the load on the pump.

During, build-up to the steady state, membrane capacitances and ionic compartmental capacitances (all non-pumped ionic compartmental capacitances are lumped with the membrane capacitance in Fig. 8 to simplify the diagram) are charged in accordance with the principles mentioned earlier. If the system is closed and reaches a steady state, the load on the pump is a function of the load presented by the parallel combination of proton leakage currents and proton currents through the potassium antiporters. The load

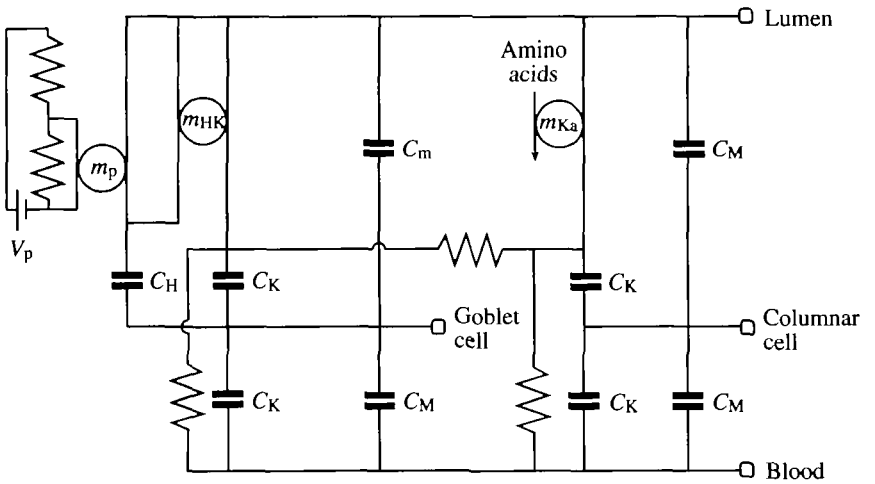

Fig. 8. Simplified diagram of midgut epithelium showing the path of potassium current through both goblet cell and columnar cell.

contributed by the antiporter is a function of the net resistance of the potassium circuit. Also, the size of the various membrane capacitances and ionic compartmental capacitances will not affect the steady-state load on the pump in any way, except as compartmental pH, transmembrane potential or the like can activate or inhibit membrane channels in the pumped or ported circuits.

However, no real biological system is ever closed. For the living insect larvae, the materials in the gut lumen and the materials in the blood are constantly in flux. In the gut and the interstitial fluids, fresh material is constantly being added and old material is being removed, giving these compartments a very large effective capacity and preventing them from becoming fully charged. Under these conditions, the steady state is like a sustained transition state. Currents would constantly be flowing in non-pumped and non-ported ionic pathways and, to the extent that these currents were a function of the pump/porter system, the magnitudes of their pathway conductances and capacitances would affect the loading on the pump.

Future directions

Viewing the energy distributions in membranes as functions of the voltage, current, capacitance and resistance parameters of the pumps, porters, channels, membranes and compartments of the system presents an opportunity to write and use computer programs like those successfully used in electrical and electronic engineering. These programs allow investigators and students to study how different circuit configurations can quantitatively affect the operation of a system. Circuit analysis programs able to handle the ionic systems of unit and epithelial membranes must include provisions for d.c. transformers of pumps and porters and provisions for handling the ionic compartmental capacities. They must also be able to handle the inherent nonlinearity of the compartmental capacitances and other components and the nonlinearities on circuit components affected by protein conformational changes in response to membrane potential, pH or ionic strength.

Another possible line of study with ionic circuit analysis is to consider the possible role of impedance matching between various ionic circuits on fitness of the organism to its environment and behavior. Maximum power delivered to a load is achieved when the impedance of the load is equal to the internal impedance of the power supply circuit. Whether the loads put on pumping circuits are relatively steady, as may be the case with the constantly eating larva of the tobacco hornworm *Manduca sexta*, or periodic, as is the case for the gypsy moth *Lymantria dispar*, which eats in spurts (M. G. Wolfersberger, personal communication), the matching of the energy demand to the energy supply would seem to be important. d.c. circuit analysis techniques described here could easily handle conditions in which the loads are constant. Varying loads in capacitative circuits introduce phase differences between the currents in the different ionic circuits that must be considered. In circuit analysis terminology such varying loads are called reactive loads. With periods of hours, days or perhaps weeks and months, matching the reactive loads to the energy distribution system would require circuits with very large capacitors such as the ionic compartmental capacitances described here. It would be interesting to

study the degree to which evolutionary processes have selected for impedance matching as an energy optimizing strategy.

Appendix 1. Determination of change in equilibrium potential with a movement of ions from one compartment to another

The equilibrium potential before (Eb_k) the transfer is:

$$Eb_k = \frac{\boldsymbol{RT}}{Z_k F} \times \ln \frac{Ni_k}{No_k}. \tag{1.1}$$

The equilibrium potential after (Ea_k) the transfer is:

$$Ea_k = \frac{\boldsymbol{RT}}{Z_k F} \times \ln \frac{Ni_k + dN_k}{No_k - dN_k}. \tag{1.2}$$

The change in the equilibrium potential caused by the transfer is:

$$dE_k = Ea_k - Eb_k. \tag{1.3}$$

Substituting equations 1.1 and 1.2 into equation 1.3:

$$dE_k = \frac{\boldsymbol{RT}}{Z_k F} \times \ln \frac{Ni_k + dN_k}{No_k - dN_k} - \frac{\boldsymbol{RT}}{Z_k F} \times \ln \frac{Ni_k}{No_k}. \tag{1.4}$$

On rearranging:

$$dE_k = \frac{\boldsymbol{RT}}{Z_k F} \times \ln \frac{No_k \times (Ni_k + dN_k)}{Ni_k \times (No_k - dN_k)}. \tag{1.5}$$

Equation 1.5 is the same as equation 7 in the text.

Appendix 2. The series combination of ionic compartmental capacitances

Two capacitors in series combine to give the following equation:

$$Ct_k = \frac{Co_k \times Ci_k}{Co_k + Ci_k}. \tag{2.1}$$

In the text it was shown that:

$$Co_k = \frac{F^2}{\boldsymbol{RT}} \times Z_k^2 \times No_k \tag{2.2}$$

and

$$Ci_k = \frac{F^2}{\boldsymbol{RT}} \times Z_k^2 \times Ni_k. \tag{2.3}$$

Let

$$U = \frac{F^2}{\boldsymbol{RT}} \times Z_k^2. \tag{2.4}$$

Substituting the appropriate capacitance equations into equation 2.1 and using the equivalence of equation 2.4:

$$Ct_k = \frac{U \times No_k \times U \times Ni_k}{(U \times No_k) + (U \times Ni_k)}. \tag{2.5}$$

Rearranging and canceling:

$$Ct_k = U \times \frac{No_k \times Ni_k}{No_k + Ni_k} \tag{2.6}$$

or:

$$Ct_k = \frac{F^2}{RT} \times Z_k^2 \times \frac{No_k \times Ni_k}{No_k + Ni_k}. \tag{2.7}$$

Equation 2.7 is the limit of equation 9 in the text.

Appendix 3. Porter coupling considerations

From the power law we know that:

$$P = IE. \tag{3.1}$$

So, from equation 1:

$$I_{in} \times E_{in} = I_{out} \times E_{out}. \tag{3.2}$$

Rearranging:

$$I_{in}/I_{out} = E_{out}/E_{in}. \tag{3.3}$$

Therefore, substituting equation 2 in the text:

$$m = E_{out}/E_{in}. \tag{3.4}$$

From the power law, we also know that:

$$P = I^2R. \tag{3.5}$$

So, from equation 1 in the text:

$$I_{in}^2 \times R_{in} = I_{out}^2 \times R_{out}. \tag{3.6}$$

Rearranging:

$$I_{in}^2/I_{out}^2 = R_{out}/R_{in}. \tag{3.7}$$

Therefore, substituting equation 2 in the text:

$$m^2 = R_{out}/R_{in}. \tag{3.8}$$

Appendix 4. Minimal value of coupling coefficient required to alkalize a compartment

From equation 24:

$$E_M = \text{pmf} \times \frac{Ct_H + (m_{HK} \times Ct_K)}{Ct_H + C_M + Ct_k + Ct_K}. \tag{4.1}$$

From equation 26:

$$E_H = E_M - \text{pmf}\,. \tag{4.2}$$

Substituting equation 4.1 into equation 4.2:

$$E_H = \text{pmf} \times \frac{Ct_H + (m_{HK} \times Ct_K)}{Ct_H + C_M + Ct_k + Ct_K} - \text{pmf}\,. \tag{4.3}$$

Rearranging:

$$E_H = \text{pmf} \times \left[\frac{Ct_H + (m_{HK} \times Ct_K)}{Ct_H + C_M + Ct_k + Ct_K} - 1 \right]\,. \tag{4.4}$$

Alkalization of the inside compartment with respect to the outside compartment results when:

$$E_H > 0\,. \tag{4.5}$$

In order for this to occur, it is necessary that:

$$\frac{Ct_H + (m_{HK} \times Ct_K)}{Ct_H + C_M + Ct_k + Ct_K} > 1\,. \tag{4.6}$$

Rearranging:

$$Ct_H + (m_{HK} \times Ct_K) > Ct_H + C_M + Ct_k + Ct_K\,, \tag{4.7}$$

$$m_{HK} \times Ct_K > C_M + Ct_k + Ct_K\,, \tag{4.8}$$

$$m_{HK} > \frac{C_M + Ct_k}{Ct_K} + 1\,. \tag{4.9}$$

Equation 4.9 is the same as equation 28 in the text.

This research has been supported in part by Faculty Incentive Grants and Faculty Development Grants from Immaculata College to F. G. M. and by NIH Research Grant AI-22444 to William R. Harvey. I wish to thank my colleagues at Temple University, Dr William Harvey, Dr Michael Wolfersberger and Dr Ranganath Parthasarathy for keeping me abreast of the current trends in transport physiology and the role of V-ATPases and, along with Dr Allan Koch of Washington State University, for reviewing this work and making many helpful suggestions. Finally, I thank Mr Daniel J. Harvey for his help in preparing the figures for publication.

References

EDMINISTER, J. A. (1965). *Theory and Problems of Electric Circuits.* New York: Schaum Publishing. 289pp.

FINKELSTEIN, A. AND MAURO, A. (1963). Equivalent circuits as related to ionic systems. *Biophys. J.* **3**, 215–237.

HARVEY, W. R. (1992). Physiology of V-ATPases. *J. exp. Biol.* **172**, 1–17.

HODGKIN, A. L. AND HUXLEY, A. F. (1952). A quantitative description of membrane current and its application to conduction and excitation in nerve. *J. Physiol., Lond.* **117**, 500–544.

HODGKIN, A. L. AND KEYNES, R. D. (1955). Active transport of cations in giant axons from *Sepia* and *Loligo*. *J. Physiol., Lond.* **128**, 20–60.

KISHIMOTO, U., KAMI-IKE, N. AND TAKEUCHI, Y. (1981). A quantitative expression of the electrogenic

pump and its possible role in the excitation of *Chara* internodes. In *The Biophysical Approach to Excitable Systems* (ed. W. J. Adelman and D. E. Goldman), pp. 165–181. New York: Plenum Press.

LÄUGER, P. (1991). *Electrogenic Ion Pumps*. Sunderland, Massachusetts: Sinauer Associates. 313pp.

MARTIN, F. G. AND MOTE, M. I. (1980). An equivalent circuit for the quantitative description of inter-receptor coupling in the retina of the desert ant *Cataglyphis bicolor*. *J. comp. Physiol.* **139**, 277–285.

MOFFETT, D. AND KOCH, A. (1992). Driving forces and pathways for H^+ and K^+ transport in insect midgut goblet cells. *J. exp. Biol.* **172**, 403–415.

SNELL, F. M., SHULMAN, S., SPENSER, R. P. AND MOOS, C. (1965). *Biophysical Principles of Structure and Function*. Reading, MA: Addison-Wesley Publishing. 390pp.